Thermal Spray 2009: Proceedings of the International Thermal Spray Conference
B.R. Marple, M.M. Hyland, Y.-C. Lau, C.-J. Li, R.S. Lima, G. Montavon, editors, p 409-414
DOI: 10.1361/cp2009itsc0409

Phase Formation in Alumina/YSZ Nano-Composite Coating Deposited by Suspension Plasma Spray Process

F. Tarasi, M. Medraj*, A. Dolatabadi
Concordia University, Montreal, Quebec, CA
**E-mail: mmedraj@encs.concordia.ca*

J. Oberste-Berghaus, C. Moreau
National Research Council of Canada-Industrial Material Institute, Boucherville, Quebec, CA

Abstract

Suspension Plasma Spray process is used for deposition of pseudo eutectic composition of alumina-yttria stabilized zirconia as a potential thermal barrier coating. Process variables including feed and process parameters were altered to find the influential parameters on the formation of phases in the composite coating. The most significant variable was recognized to be the plasma auxiliary gas. It influences the formation of the crystalline and non-crystalline phases by affecting the resulting in-flight particle state, mainly the particle velocity.

Introduction

Alumina-zirconia coatings are being considered as potential alternatives to the present thermal barrier coatings (TBCs). The TBCs include cubic or tetragonal zirconia stabilized by substituting some of the Zr atoms with one or more of the base elements from alkali metal oxides like CaO, MgO, transient metal oxides as in Y_2O_3, Sc_2O_3, Er_2O_3 (Ref 1) or rare-earths such as CeO, Yb_2O_3, or the whole Lanthanides group (Ref 2). Stabilization is to prevent the adverse effects of the phase transformation of zirconia coatings into monoclinic structure. Alumina seems to be a proper mix in the composite with zirconia that can enhance its thermodynamic stability (Ref 3-5) at various temperatures, improves its mechanical properties (Ref 6), and thermal resistivity (Ref 7).

Each of zirconia and alumina during deposition by plasma spraying has its own phase formation behavior. According to Golozar *et al.* (Ref 8), as deposited YSZ coating applied by atmospheric plasma spray (APS) process shows mainly tetragonal, sometimes with some cubic structure. Alumina, on the other hand, presents the cubic γ crystal structure regardless of the plasma spray technique and powder feed size (Ref 9-12) except for the case of nano powder feed that has ended with mainly hexagonal α structure in conventional plasma spray (Ref 13). In alumina-YSZ composites besides the amorphous phase some times reported (Ref 14), almost the same crystalline structures as in each individual coating were observed. That means the YSZ is mostly tetragonal, in addition to sometimes some cubic structure and the alumina appears as γ phase (Ref 6, 14-16).

The above mentioned studies focus on a few specific spray conditions in concerning processes. However, in each spray process under various spray conditions, formation of different phases is possible. The purpose of this study is to determine the effective variables on the crystalline phase formation in the suspension plasma sprayed coatings of the pseudo eutectic composition of alumina-8wt%YSZ composite. The feed material and process parameters in suspension plasma spray process were varied to enable the prediction of the phase analysis under each spray condition.

Experimental

A group of 16 samples were coated on (2.5×2.5×0.5 cm^3) mild steel coupons using suspension plasma spray (SPS) process. Powder feeds with weight ratio of 60 alumina / 40 yttria stabilized zirconia (YSZ) were deposited under various spray conditions. To produce two different powder size ranges, first 5 wt.% YSZ and 13 wt.% YSZ powders, both with a size distribution of 30-60 nm (from Nano-Composite Powder, Inframat @ Advanced Materials, Farmington, CT, USA) were proportionally mixed, to produce 8 wt.% YSZ. The resulting doped zirconia combination was then mixed with two different sizes of alumina powders. The alumina component was nano with a nominal size of 27-43 nm (Nanostructured & amorphous Materials Inc., Los Alamos, New Mexico, USA) or micron with an average size of 1.4 μm (Baikowski Malakoff, Malakoff, TX, USA). The resulting mixtures were called “Nano” and “Micron”, respectively. According to the initial assessment of XRD patterns from each of the used powders in this experiment, the zirconia nanopowder consists of cubic structure and the alumina naopowder contains both rhombohedral (α) and cubic (γ) structure. The ratio of α/γ,

according to the supplier, is equal to 95/5 wt.%, while the micron size alumina powder shows only α structure. The loose nano and or micron size powders were mixed and suspended in ethanol as the carrier liquid for injection of the solid feed into plasma torch. 8YSZ nanopowder was also deposited individually using the same process as a reference point and to investigate the preferred crystalline structure of the material outside the composite.

The variables studied in this work are listed in Table 1. They consist of plasma spray condition such as the plasma auxiliary gas and the feed related parameters consisting of solid content in the suspension, feed rate and the powder size range. The last column of Table 1, also, indicates the plasma powers resulted from the auxiliary gas change and variation of other spray conditions described in details in (Ref 17). The variables were changed in two levels that can be extracted from the same table. The resulting in-flight particle velocity and temperature were monitored by diagnostic system Accura-Spray G2 (Tecnar Automation, St. Bruno, QC, Canada). Since the small particle size does not let the individual measurements, the system monitors the ensemble particle velocity and temperature. The X-ray Diffraction patterns were produced using D8 Discover diffractometer (Bruker Axs Inc., Madison, WI, USA) and the relative phase amounts were calculated based on Reitveld refinement techniques using the Powdercell program (Ref 18).

Results and Discussion

The as-deposited coatings present various structures as shown in Fig.1. The investigation of the X-ray diffraction patterns in this experiment revealed that stabilized zirconia basically appears as face centered cubic structure matching with ICSD database number 82-1246, formula $Zr_{0.8}$ $Y_{0.2}O_{1.9}$ and symmetry system (225) equivalent to Fm-3m (accepted as t" structure by the data base), or number 30-1468 formula $Y_{0.15}Zr_{0.85}O_{1.93}$ with the same symmetry. This structure appears in both, stabilized zirconia in the composite with alumina and pure coating as in Fig. 1(a). The difference between the cubic and t" zirconia is in the oxygen anions displacements within the structure (Ref 1) so that in t" structure there is a slight displacement from tetrahedral interstitial positions for oxygen atoms as compared with the so called "cubic structure". In a group of the samples however slight splitting of the peaks at about 59-60°, as in Fig. 2, that are related to the planes (103) and (211) of tetragonal structure, approves the presence of some tetragonal YSZ phase compatible with ICSD database number 82-1242 and formula $Zr_{0.88}$ $Y_{0.12}O_{1.94}$. In general, the dominant structure for zirconia in this experiment was mainly cubic (or t") structure.

It was noticed, in case of alumina, that the majority of the coatings deposited using helium auxiliary gas (samples number 1 to 5 in Table 1) in XRD test shown in Fig. 1(b) were matching with the α–Al_2O_3 with rhombohedral (hexagonal) structure known as corundum with ICSD number 71-1123,

Table 1: Variables evaluated for the effect on phase formation.

Sample number	Auxiliary Gas	Solid Content	Feed rate (kg/h)	Powder Type	Power (KW)
1	He	30%	1.8	Nano	57
2	He	30%	1.8	Micron	57
3	He	10%	1.8	Micron	57
4	He	30%	1.3	Nano	56
5	He	10%	1.3	Nano	82
6	H_2	30%	1.3	Micron	84
7	He	30%	1.3	Micron	81
8	H_2	30%	1.3	Nano	118
9	H_2	10%	1.3	Micron	117
10	H_2	30%	1.8	Nano	118
11	H_2	10%	1.8	Micron	116
12	He	10%	1.3	Micron	80
13	H_2	10%	1.3	Nano	85
14	H_2	30%	1.8	Micron	85
15	He	10%	1.8	Nano	82
16	H2	10%	1.8	Nano	85

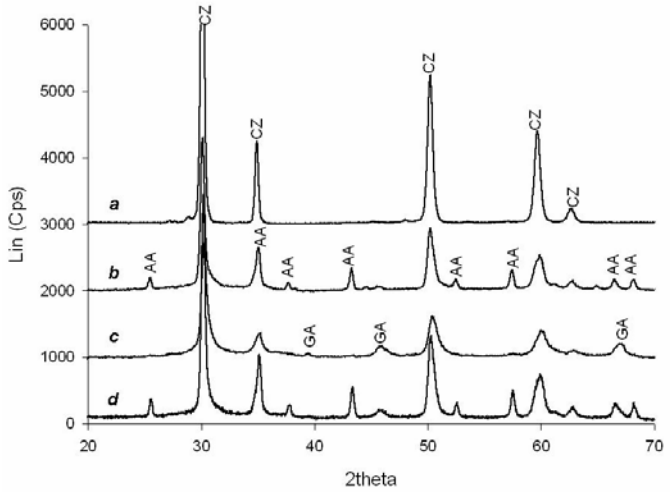

Figure 1: Typical XRD patterns from SPS deposition of 60Al_2O_3/40YSZ under various spray conditions showing cubic zirconia (CZ) in a) 8YSZ and all other crystal structures and b) sample with α- alumina (AA) as the major alumina phase ; or c) γ-alumina (GA) as the major alumina phase; d) mixed of both GA and AA alumina in addition to cubic zirconia.

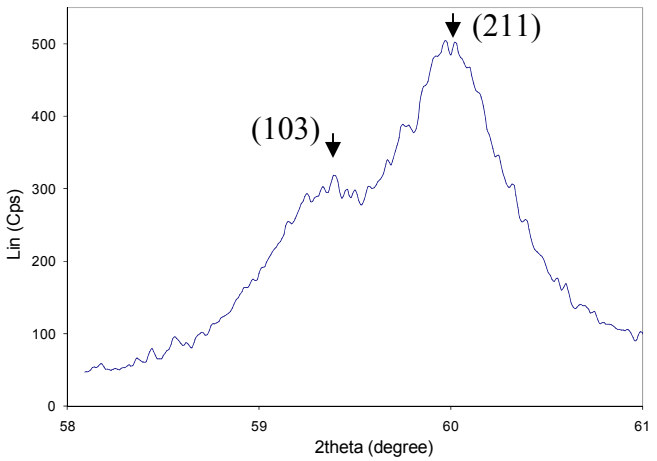

Figure 2: Peak splitting as an indication of tetragonal zirconia phase formation and the concerning planes to each peak.

formula Al_2O_3 and symmetry system (167) equivalent with R-3c.This is while in most cases (samples 6 and 8~12 in Table 1), application of hydrogen auxiliary gas ensued the formation of γ-Al_2O_3 phase with face centered cubic (FCC) structure matching with ICSD data base number 75-0921, formula $(Al_2O_3)_{1.33}$ and symmetry system (225) equivalent with Fm-3m symmetry. Figure 1(c) represents this crystal structure consisting of cubic YSZ and γ-Al_2O_3.

As a result, among the variables in this experiment, plasma auxiliary gas seems to be of major influence on the phase formation in as deposited coatings. It is worth to recall that plasma auxiliary gas was recognized as the most important variable on the particle velocity as the authors reported in (Ref 17). Besides, the same study showed the dependency of the velocity on the plasma power. The correlation between the particle state and the resulting crystalline phases within the coating are illustrated in Fig. 3. In this figure, the coatings with only γ-Al_2O_3 are shown as round symbols and the square points are representative of the coatings with only α-Al_2O_3. It is evident from this figure that at lower particle velocities (*i.e.* below 650m/s), α-Al_2O_3 was formed; while at higher velocities (*i.e.* above 730 m/s) the dominating phase is γ-Al_2O_3. Meanwhile, the tetragonal peaks in zirconia structure (not shown in Fig. 3) were normally observed within the coatings from lower velocity particles.

Typical SEM crystal structures of the coatings at high and low particle velocities are shown in Fig. 4. It is apparent in Fig. 4(a) that higher velocities have caused wider splat spreading. This is expected because the particles with higher velocities flatten faster (Ref 19), therefore the flattening process happens before the start of solidification (Ref 20) and the crystalline phase formation. Meanwhile, thinner splats with larger effective contact area in the intersplat and substrate interfaces could be of great importance on phase formation. They can help higher cooling rates, as it has been reported that the

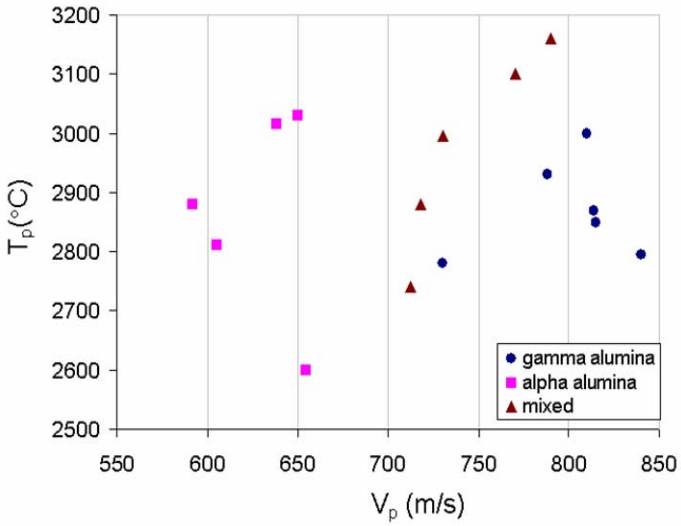

Figure 3: Alumina component phase formation behavior within the as deposited composite versus the in-flight particle state.

thermal contact resistance and splat thickness strongly affect the cooling rate (Ref 21). Higher cooling rates are shown to be in favor of metastable phases like γ-Al_2O_3, basically because of the lower liquid-solid interfacial energies with the nucleation surface which promotes higher kinetics and the formation of these phases due to smaller energy barrier for nucleation (Ref 21, 22). This explanation for alumina can be generalized to zirconia splats in which more stable phase, tetragonal zirconia, has appeared in the case of coatings with lower cooling rates and lower particle velocities, while the cubic phase could have solidified at higher cooling rates (Ref 23). In this regard, the role of unmolten or semi-molten nanoparticles entrapped in the molten particles should not be ignored.

Figure 5 presents a large in-flight solidified particle within the coating illustrating such entrapment. The round edges of the particle show that it is resolidified. However, the particles shown by the arrow in the center have remained unmelted. These particles at low particle velocities when in-flight solidification happens, can play a pronounce role as the nucleation sites. Therefore in a structure with enormous number of in-flight solidified particles, as in Fig. 4(b), there are higher chances of formation of the initial structure of the feed powder. This fact causes more complications in prediction of the resulting structure.

Intermediate velocities, shown by triangles in Fig. 3, present a mixed structure of γ and α alumina in addition to cubic zirconia along with different amounts of tetragonal zirconia. This kind of structure can be seen in the XRD pattern of Fig. 1(d). A dependency among the present phases in the coating was found in Fig. 6. This figure indicates the relationship between the percentages of γ phase in alumina compared with

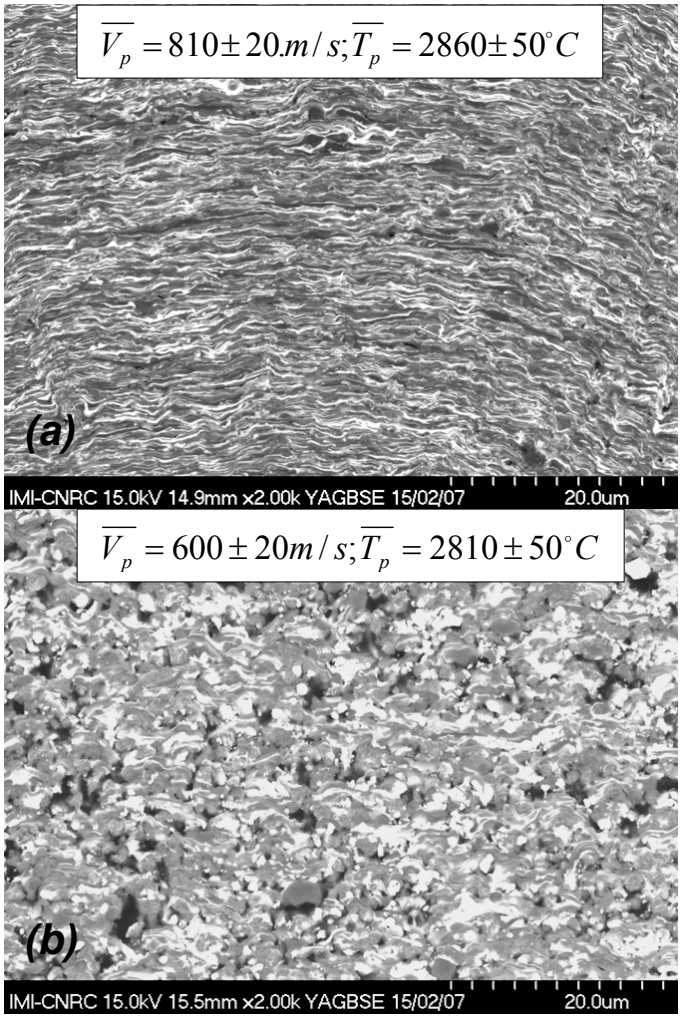

Figure 4: SEM micrographs of the coatings deposited using a) H2 gas with high particle velocities b) Helium auxiliary gas with lower particle velocities resulting in different splat flattening and intersplat contact area.

the cubic phase in zirconia component of the coating. It can be seen that the percentage of the cubic zirconia increases with increasing the γ-alumina content. This Suggests that γ-alumina formation coincides with cubic zirconia formation.

Particle temperature is dependent on feed parameters such as feed rate and solid content (Ref 17). These parameters of feed could affect the structure through changing the particle temperature. Considering the small size associated with the particles in the SPS process a comparatively uniform temperature throughout the particle mass is predictable, and the in-flight particle temperature upon impact, being high enough for complete melting of both components (usually more than 2730°C) does not seem to play any major role. The exception is that at very high particle temperatures (i.e. beyond 3000°C) as in the last two points of the mixed structures in Fig. 3, it appears to result in formation of some α-alumina phase at high velocities, where only γ phase is

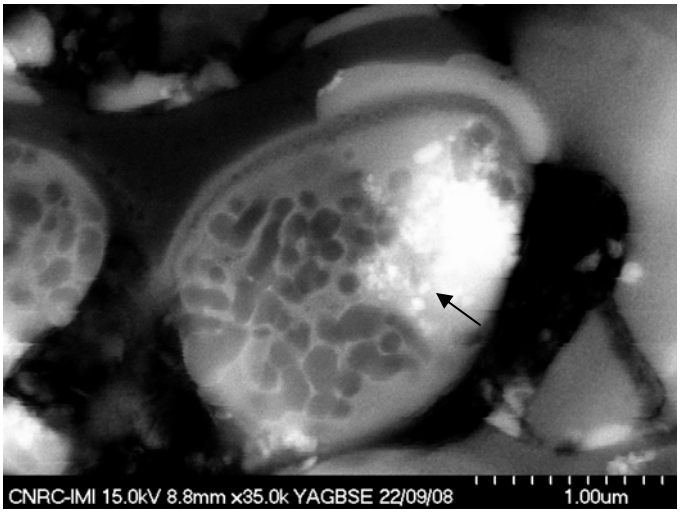

Figure 5: Entrapped unmolten nanoparticles inside the large in-flight solidified particle in the coating.

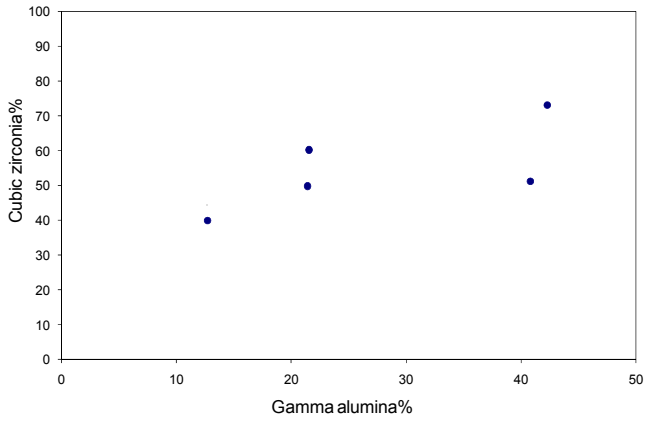

Figure 6: The correlation between the gamma percentage in alumina and the cubic phase percentage in zirconia showing the coincidence of the appropriate condition for formation of both phases.

expected. In this case, impingement of overheated particles on the substrate contributes to excessive heating of the coating and consequently the formation of α alumina phase (Ref 22). In addition, reheating the coating by the following deposition passes of the hot particles has caused more formation of α out of metastable γ-alumina.

Variation in phase contents is expected with changes in other variables of Table 1 such as, particle temperature and feed size, which have not shown any major effect on the nature of the present phases in this experiment. Focusing on the group of samples with mixed structure, Fig. 7 shows the relationship between the γ phase percentages and the particle velocity in this group. In this figure the points are indicated by the sample number as mentioned in Table 1, also to help the comparisons, the particle temperature and the feed size range are added to

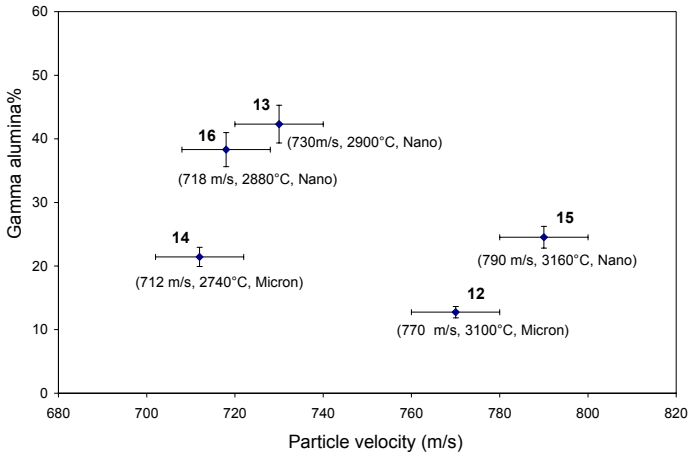

Figure. 7: The percentage of γ-alumina in alumina phase versus particle velocity in the samples with mixed structure showing the role of Particle temperature and feed size range.

the figure. Comparing samples 13, 14 and 16 (left side) with samples 12 and 15 (right side) in Fig. 7, verifies the effect of high temperature on phase formation. The figure shows how, in spite of that higher particle velocities predict higher γ ratios, too high particle temperatures in samples 12 and 15 have pursued almost equal or even smaller amounts of γ phase compared with the coatings of lower particle velocities. On the other hand, the minimum amounts of γ-alumina phase are observed in samples 12 and 14 that as per table 1 are related to the coatings from the micron size powders, while samples 13, 15 and 16 are produced by the nanopowder feed material. Larger particle size forms thicker splats that decreases the cooling rate and facilitates the formation of more stable phases like α-alumina.

Conclusion

In this experiment with pseudo-eutectic alumina-YSZ coatings using SPS process, plasma gas composition seemed to be the most important variable in phase determination. Relying on the previous studies on the roles of the plasma gas, it appeared that this effect prevails through the variation of the in-flight particle velocity. Particle temperature, as long as it is high enough for complete melting of the particles, does not play an explicit role in nature of the present phases. It, however, can affect the phase contents. Feed size, also, changes the phase contents, so that the larger particles result in formation of more stable phases in the coating. Other feed parameters including feed rate and solid content influence the results through variation of the particle temperature. The presence of unmolten nanoparticles increases the intricacy of the phase prediction in as deposited coating.

References

1. M. Yashima, M. Kakihana, and M. Yoshimura, Metastable-Stable Phase Diagrams in the Zirconia-Containing Systems Utilized in Solid-Oxide Fuel Cell Application., *Sol. Oxide Ionics*, 1996, **86**, p1131-1149
2. C.G. Levi, Emerging Materials and Processes for Thermal Barrier Systems, *Current Opinion in Sol. State and Mat. Sc.*, 2004, **8**(1), p77-91
3. H.S. Kurt, *Metallurgical and Ceramic Protection. Coatings*, Chapman & Hall, UK,1996, p194-229
4. E. Djurado, P. Bouvier, and G. Lucazeau, Crystallite Size Effect on the Tetragonal-Monoclinic Transition of Undoped Nanocrystalline Zirconia Studied by XRD and Raman Spectrometry, *J . Sol. State Chem.*, Feb.2000,**149** (2), p399-407
5. M. Andritschky, I. Cunha,and P. Alpuim, Thermal Stability of zirconia/alumina Thin Coatings Produced by Magnetron Sputtering, *Surf. & Coat. Tech.*,1997,**94-95** (1-3), p144-148
6. A.M. Limarga, S. Widjaja, and T.H. Yip, Mechanical Properties and Oxidation Resistance of Plasma-Sprayed Multilayered Al2O3/ZrO2 Thermal Barrier Coatings, *Surf. & Coat. Tech.*,2005/7/1,**197** (1) , p93-102
7. P. Ramaswamy, S. Seetharamu, K.B.R. Varma, and K.J. Rao, Al_2O_3/ZrO_2 Composite Coatings for Thermal-Barrier Applications, *Comp. Sci.& Tech.*,1997,**57** (1) , p81-89
8. M. A. Golozar, J. Mostaghimi, T. W. Coyle, and R. Soltani, Wear Behavior of Nanostructured and Conventional Y-PSZ Coatings, *International Symposium on Materials Degradation: Innovation, Inspection, Control and Rehabilitation*, 21-24 Aug. 2005,(Calgary, AB, Canada), 2005, p273-285
9. R.J. Damani, P. Makroczy, Heat Treatment Induced Phase and Microstructural Development in Bulk Plasma Sprayed Alumina, *J. the Eur. Ceram. Soci.*, June 2000,**20**(7), p867-888
10. K.S. Ravichandran, K. An,and R.E. Dutton, and S.L. Semiatin, Thermal Conductivity of Plasma-Sprayed Monolithic and Multilayer Coatings of Alumina and Yttria-Stabilized Zirconia, *American Ceram. Soci.*,1999, **82**(3), p673-682
11. Strangman, E. Thomas, Raybould, Derek, durable thermal barrier coatings, U.S. patent No. 20060115660, 2006
12. Zun Chen, R.W. Trice, M. Besser, Xiaoyun Yang,and D. Sordelet, Air-Plasma Spraying Colloidal Solutions of Nanosized Ceramic Powders, *J. Mat. Sci.*, 2004, **39**(1), p4171-4178
13. Y. Zeng, C. Ding, and S. Lee, plasma Sprayed Coatings using Different Nanosize Alumina Powders., *Thermal Spray 2003: Advancing the Science and Applying the Technology, International Thermal Spray Conference*, May 2003,(Orlando, FL, United States), 2003, p671-674
14. J. Oberste-Berghaus, J.-G. Legoux, C. Moreau, F. Tarasi, and T. Chraska, mechanical and thermal transport properties of suspension thermal sprayed alumina-zirconia composite coatings, *J. Therm. Spray Tech.*, **17**(1),Mar.2008, p91-104
15. Skoog, A. Jay, Murphy, A. J., Tomlinson, and T. John, method for applying a plasma sprayed coating using liquid injection, U.S. Patent No.20060222777, 2006

16. A.L. Vasiliev, N.P. Padture, and X. Ma, Coatings of Metastable Ceramics Deposited by Solution-Precursor Plasma Spray: I. Binary Al_2O_3-ZrO_2 System, *Acta Materialia*, Oct.2006,**54**(18), p4913-4920
17. F.Tarasi, M. Medraj, A. Dolatabadi, J. Oberste-Berghaus, and C. Moreau, Effective Parameters in Axial Injection Suspension Plasma Spray Process of Alumina-Zirconia Ceramics, *J. Therm. Spray Tech.*,2008 (in press)
18. Powdercell for windows (computer program), Werner Kraus and Gert Nolze, Version 2.4, 8/3/2000, http://www.ccp14.ac.uk
19. H. Zhang, X.Y. Wang, L.L. Zheng, and S. Sampath, Numerical Simulation of Nucleation, Solidification, and Microstructure Formation in Thermal Spraying, *Intern. J Heat and Mass Transf.*,2004, **47**, p2191-2203
20. A. Haddadi, F. Nardou., P. Fauchais, A. Grinaud, and A. C. Leger. , Influence of Substrate and Coating Temperature on Columnar Growth within Plasma Sprayed Zirconia and Alumina Coatings, *United forum for scientific and technological advances*, C. C. Berndt, Ed., ASM International,1997, p671-680
21. P. Fauchais, M. Vardelle, A. Vardelle, L. Bianchi, and A.C. Leger, Parameters Controlling the Generation and Properties of Plasma Spray Zirconia Coatings, *plasma chem.& plasma proc.*, Mar. 1995,**16**(1), pS99-S125
22. A. Vardelle, C. Robert, G.X. Wang, and S. Sampath, Analysis of Nucleation phase Selection and Rapid Solidification of an Alumina Splat, *Thermal Spray: A United Forum for Science and Technological Advances*, C.C. Berndt, Ed.,1997, ASM International, p635-643
23. Chraska T., King A.H, Transmission Electron Microscopy Study of Rapid Solidification of Plasma Sprayed Zirconia-Part II. Interfaces and Subsequent Splat Solidification, *Thin Film Sol.*, 2001, **397**, p40-48